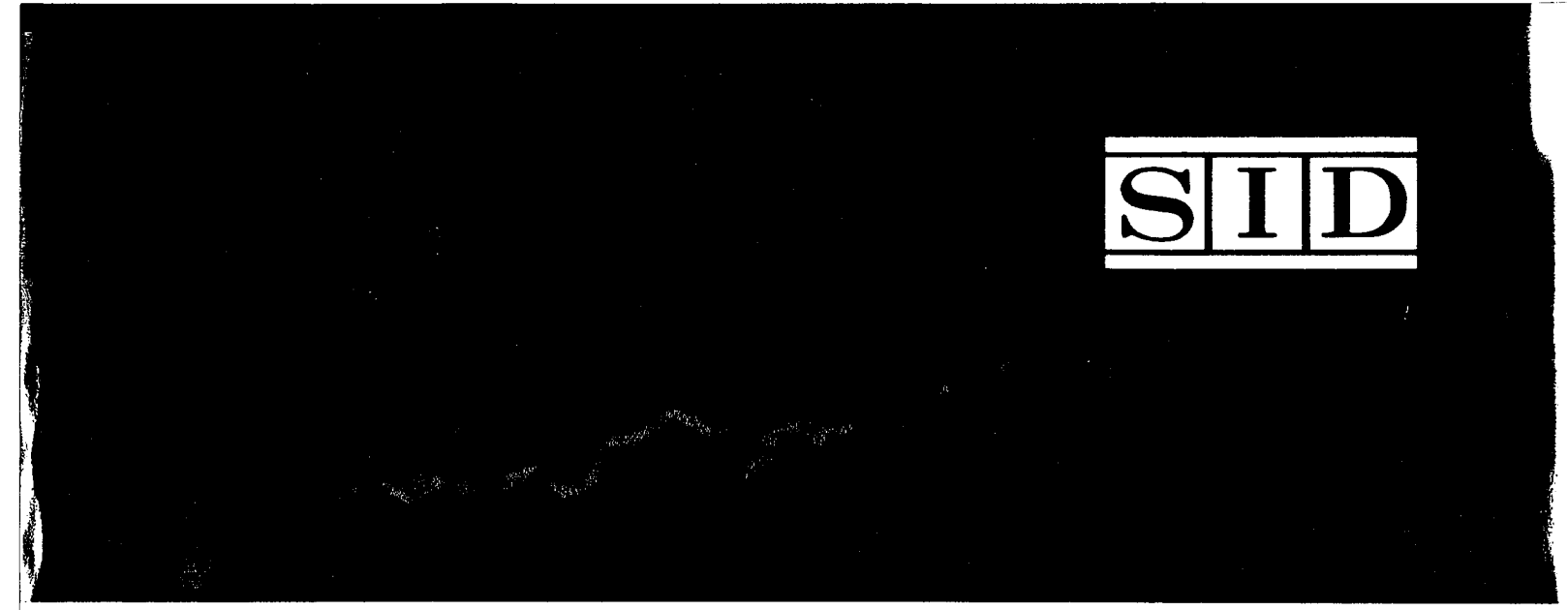

SOCIETY FOR INFORMATION DISPLAY

INTERNATIONAL SYMPOSIUM

DIGEST OF TECHNICAL PAPERS

VOLUME XXIII

HYNES CONVENTION CENTER
BOSTON, MASSACHUSETTS
MAY 17-22, 1992

Session 16

Visual Factors in Virtual-Image Displays

Chair
Brian H. Tsou
AAMRL

Co-Chair
Robert C. Carter
Naval Research Laboratory

Many visual factors can affect the design of head-mounted virtual image displays (VIDs). Some of these factors will be discussed in this session.

The first paper will provide an overview of the human binocular fusion demands that may specifically drive the VID collimation requirement. The accuracy of ocular accommodation will be compared for binocular versus monocular viewing. The second paper will discuss the interrelationship between the display field-of-view (FOV) and peripheral vision. The study is based on human ability in vehicle control and roll-motion perception. The third paper will illustrate, using a novel VID design as an example, that the visual psychophysical cue for space judgment can be adversely affected by the typical optical design of a night-vision goggle. The theory behind the new VID will be presented. The fourth paper will show how the involvement of ambient vision with a wide FOV display can enhance the subject's spatial awareness. The fifth and final paper will present data to show that size perception is not affected by ocular dominance and that learning plays a significant role.

These presentations will demonstrate that in order for a VID to be usable, visual perception must be considered early in the design stage.

16.2: Human Performance and Field of View

R. V. Kenyon
University of Illinois, Chicago, IL
E. W. Kneller
Chase Naval Air Station, Tx

Abstract

The affects of different field of view (FOV) sizes on human performance during a critical tracking task are presented. The critical tracking task is used to measure changes in the subjects' effective time delay for different FOV configurations. Performance in stabilizing the roll motion of a visual scene driven by an unstable first order plant is worst at a 10° FOV condition. The best performance occurs at 80° or 120° FOV sizes. These results provide a quantitative basis for choosing a FOV size in a visual display system. The impact of these FOV conditions on human workload and visual function will be discussed.

Background

Manual control paradigms and methodologies provide a means by which one can mathematically describe some portion of human performance (usually the linear part of the system). Manual control theory has been used for many years to describe, in a quantitative manner, the man-machine interaction with a control system [10]. The manual control approach circumvents less satisfying methods that do not lead to an equation that can be used to describe the operator. Once the human operator model is identified, it can be used in the control equations for any external control system and allow the evaluation of how that overall system (human and machine) will perform [8]. Such models also allow prediction of behavior not tested and can lead to new experiments to examine human performance.

Vision Characteristics

The human visual system provides information used to identify objects as well as information about our orientation [3]. The fovea, a 2° diameter area of the central retina that can resolve a 1 min arc separation, is used in reading, and other tasks that require detail from objects in our field of view (FOV). Using the extraocular muscles, the fovea can be aimed at any object in the FOV. While not usually used to provide orientation information, some perceptions of linear motion have been elicited from this area [1].

The major component of our visual spatial orientation sense is provided by the peripheral retina which extends radially from ±15° to the edge of the field of view ±90°. While poor at providing high spatial frequency information about an object's characteristics and detail, this area of the retina processes low spatial frequency information and motion that is used to generate our sense of spatial orientation. Wide field of view presentations of tilted rooms and other such scenes have been shown to lead to errors in perception of vertical [6].

Vection

Illusions of self-motion (vection) both angular (circular vection) and linear (linear vection) are in large part due to the processing of visual information by the peripheral visual system [2]. Motion of a visual scene can elicit a perception of motion even when the vestibular system's signal has decayed away. For example, a passenger sitting in a stationary train will feel motion when an adjacent train (seen in the passenger's peripheral visual field) slowly moves outside the window. Studies in animals have shown that information from the vestibular system and the peripheral visual field converge at a common center in the brain (the vestibular nucleus) [13]. This convergence takes place at such a fundamental level in processing of motion information that it is believed to be the reason that vection and real motion are hard to distinguish.

Control of Roll Motion

Shirley and Young [12] showed that human operator performance can be greatly enhanced by the adding veridical motion stimuli to the subject during a roll control task. Their results showed that the stimulation of the vestibular system provided additional phase lead to the human operator. When this study is considered in light of the work of Dichgans and Brandt [2] and Waespe and Henn [13] (see above), it becomes important to know if wide FOV motion stimuli can provide the same phase lead as does true motion stimuli to the human operator.

Junker and Levison [8] systematically explored the role of motion and wide FOV visual stimuli on human operator characteristics. Their studies examined roll motion and used both a nulling task and a pursuit tracking task. They found that the addition of wide FOV roll motion provided similar enhancements of human operator performance as did motion over a narrow FOV condition without motion. In the nulling task experiments, wide FOV and motion conditions showed increased crossover frequency due to addition of mid to high frequency phase lead over the narrow FOV no motion condition. In the pursuit tracking experiments with narrow FOV and no motion, the human operator transfer function showed a significant low frequency phase droop with respect to the other two conditions.

Hosman and van der Vaart [4] found similar results using a disturbance nulling task. They examined pilot performance in controlling simulated aircraft roll. In their experiment the pilot's task was to keep the aircraft roll as close to wings level (0° with respect to the horizon) as possible. The aircraft dynamics were modelled as a neutrally stable second order system. A quasi random disturbance signal was used to produce a roll error which the pilot attempted to correct. For one experimental case the subject was shown a central display alone and in another case the subject was presented with the central display and left and right peripheral displays. Measurements of the root mean square (RMS) roll error showed a significant improvement when the pilot used peripheral displays in addition to the central display. Analysis of the transfer function showed that the pilot's crossover frequency increased when the peripheral displays were added to the central display, indicating a greater stability margin.

Present Experiments

The current work extends these studies on visual vestibular interaction using manual control paradigms to examine the affects of different sized FOV on human operator performance during a fixed-based roll control task. These experiments were designed to occupy the subject with a demanding manual control task at different FOV sizes. Comparison of the performance measures and human operator parameters from the manual control responses under each FOV condition will indicate the range of FOV sizes that are optimal.

Methods

Critical Tracking Paradigm.

Theory. The CT paradigm was was developed by Jex et al. [7] to estimate the effective time delay of the human operator, t_d. The sub-

ISSN0097-0966X/92/0000-290-$1.00 + .00 © 1992 SID

ject acts as a regulator in a feedback control system which includes an increasingly unstable, first order divergent control plant:

$$Y_C = \frac{K_c}{Ts-1} = \frac{\lambda}{s-\lambda} \quad \text{where} \quad \begin{cases} \lambda & = 1/T \\ K_c & = 1.0 \end{cases} \qquad (1)$$

Although there is no external driving function, the rising instability level of the plant and the inherent noise in the human control system, makes minimizing the system's error, '*e*', increasingly difficult. At the endpoint of control, the plant instability cannot be compensated by the subject and the system's output is saturated. Jex et al. [7] showed that the plant instability level where control is lost, λ_c, is a measure of the subject's effective time delay, $t_d \approx 1/\lambda_c$.

To estimate λ_c with reasonable accuracy, the adjustment itself of λ, during a run, must not greatly influence the outcome of the experiment. If the rate used to increase λ is too high, the λ_c values may be optimistic due to λ increasing a significant amount during the moment after the subject loses control but before the display reaches its end point. A too slow an increase in λ will overly fatigue the subject.

Implementation. The CT task was adapted to these experiments by using the critical control plant as the roll dynamics of the visual scene. The subject's task was to maintain the roll error angle at 0° for as long as possible. This one-dimensional control task, forced the human operator Y_H to pilot the control element Y_C such that the error "seen" by the operator was minimum or else control would be lost. Loss of control was defined as the point where the unstable plant forced the roll angle of the scene to an unrecoverable maximum CW or CCW position (±100°).

In all experiments λ was first initialized to a low value (2.0) then increased at a relatively rapid rate $\dot{\lambda}_1$, until the subject's performance deteriorated past a predetermined level, indicating that λ was close to its critical value, λ_c. The transition from $\dot{\lambda}_1$ to $\dot{\lambda}_2$ was determined by two factors: the λ value must have been greater than 3.2 and the average absolute roll error of the display, over 2/3 second, must have been greater than 13°. If both conditions were met, then λ increased at about 1/4 its previous rate until the subject lost control. The initial fast rate, $\dot{\lambda}_2 = 0.112$ rad/sec, allowed the plant to transition from a relatively stable level to the near critical level over a short period of time (20-40 secs) thereby avoiding subject fatigue. The second rate, $\dot{\lambda}_2 = 0.03$ rad/sec, was slow enough not to overshoot λ_c.

Scene Generation

A dedicated graphics workstation (Silicon Graphics IRIS 2400) was programmed to read and store the subject's control input, and generate the out-the-window scene. The workstation displayed the scene on a 19 inch, 30 Hz interlaced, color monitor (CRT) with a resolution of 768 x 1024 red, green, and blue (RGB) pixels (over the 120°, each pixel measured 9.37 x 7.03 min. arc). The scene viewed by the subject was a stylized landscape drawn in perspective.

Viewing System.

The visual conditions were produced by having the subject view the face of the CRT through the Expanded Field Display (EFD): an optical system that expands the CRT image over a 120° field of view (Figure 1) in both horizontal and vertical axes. The heart of the EFD is the stereo viewer component of the Large Expanse Extra Perspective (LEEP) Stereoscopic Imaging System (Pop Optix Labs of Waltham, MA.)[5]. This viewer is coupled to the image on the face of the CRT using a ground glass projection screen (Rolyn Optics #55.3050) placed approximately 1 cm in front of the viewer along with a fresnel lens (f.l. = 10 cm; Rolyn Optics #16.7200) placed against the far side of the ground glass so that light from the periphery was directed towards the eye. Two 80mm projection lenses (Rolyn Optics #30.1451), producing two *duplicate* images of the CRT on the left and right half, respectively, of the ground glass, thus producing two separate and identical, side by side images. A partition that extended from between the two lenses to the ground glass screen, prevented the two images from overlapping. The particular FOV was created by cutting circular holes in 2.5 x 4 inch sections of black matte paper using the following equation [5] to calculate the radius of the opening:

$$r = M(\theta - k\theta^3) \qquad (2)$$

where θ (rad) is the FOV angle from the optical axis, r (cm) is the corresponding radial distance from the center of the image, $k = 0.22$ rad^{-2}, *and* $M = 3.7$ cm. These masks were then placed in over the ground glass to create the desired FOV.

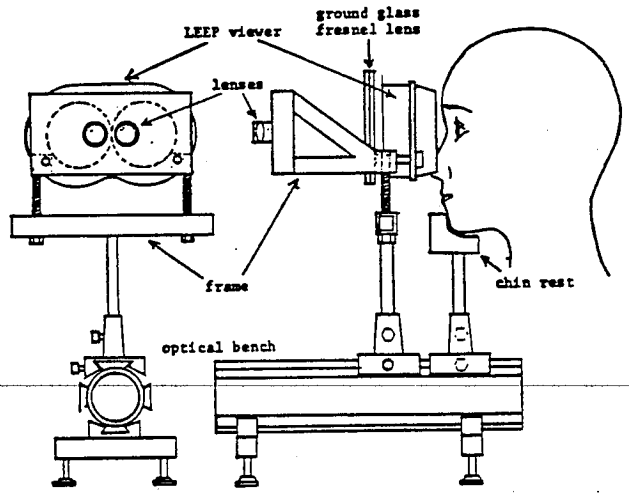

Figure 1: The wide field of view optical system used to provide the 120° FOV from the 19 inch CRT of the graphics computer.

Human Protocol

Five males in good health, free of any obvious motor coordination anomalies, and with distant vision corrected to at least 20/20; served as subjects. Subjects were trained for three days before collecting data. A simple two degree-of-freedom force-stick, used to control the *roll velocity* of the scene (Measurement Systems Model #435). was mounted securely to the right hand side of the subject's chair. A contoured armrest, also attached to the chair, was used to stabilize the forearm. Lateral force on the stick was converted to an analog voltage (±10V range) that was anti-aliased with a first-order low-pass filter with a break frequency of 3.8 Hz. This analog signal with a voltage/force ratio of 22mV/N, was then sampled at 15 Hz using an A/D card installed in the workstation (Analog Devices DT772). The sampled stick signal was converted to radians using a scale factor of 0.09 radians/N.

Every subject ran six trials: three trials per day over two consecutive days. A trial lasted approximately 20-25 minutes with a five-minute break between trials. Ordering effects on the data were minimized by balancing the presentation of the conditions within each trial.

General Data Analysis

Two time constant measurements were calculated from the data: critical and transition time constants. The 'critical time constant' is inverse of the plant instability level, ie. $1/\lambda$, when the subject loses control of the scene and represents the effective time delay of the subject. The 'transition time constant' represents the inverse of the plant instability level, $1/\lambda_t$, when $\dot{\lambda}$ changed from a high to a low value. The transition time constant serves as an indicator of task difficulty as the operator approaches λ_c.

The Stage-1 RMS values were obtained by calculating the RMS value of the first 226 roll error values of each experiment. These roll error values occur when the plant instability changes from $\lambda = 2.0$

rad/sec, to $\lambda = 3.2$ rad/sec, a total of 15.1 seconds (60-70% of the total experiment duration). Since the plant instability function during this interval was uniform in all experiments regardless of the subject's performance, these Stage-1 RMS values were compared within and across subjects at different FOV settings.

Nonparametric statistics were used to analyze the possible differences between experimental cases. A Mann-Whitney test was performed on the Stage-1 RMS and time constant values within each subject [11].

Results

The open box symbols in Figure 2 represent the mean critical time constant (T_c) values for subject A. Although each subject had a different minimum T_c value indicative of differences in their ability to perform the task, the 10° FOV produced the longest T_c in all of our subjects. An exponential-like drop in the T_c with FOV was found in subjects A, B, and E. In these subjects, a significant ($p < 0.01$) decrease in T_c from the 10° FOV condition occurred within a 40° FOV.

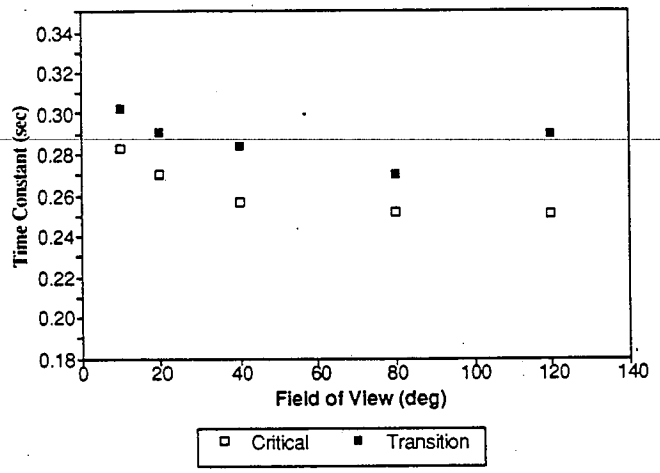

Figure 2: Average critical time constant value for subject A at the indicated Field of View.

To compare results across subjects, the mean T_c values in Figure 2 were normalized within each subject and then combined in Figure 3a. A wide FOV produced a reduction in T_c of about 10-12% in most subjects compared with a 10° FOV. Most of this improvement can be obtained with a FOV as small as 40°. The sharp decline in "effective" time delay between 10° and 40° was significant in three of the five subjects.

The filled-triangles in Figure 2 represent the mean transition time constant (T_t). The trend in this data follows a U-shaped curve (three of the five subjects) as the FOV increases with a minimum value at 80°. Comparing the mean T_c with the mean T_t, reveals a difference between the two that is larger at 120° than at the other FOVs (found in three of the five subjects: A,B,E). Such a large difference between these two time constants signifies a much higher degree of variability in the roll error at 120° than at other FOVs. In practical terms, the higher T_t values mean that the switch to the slower $\Delta\lambda$ took place sooner at 120° than, for example, at 80°. However, despite this difference, all subjects were able to achieve as good a T_c value at 120° as at 80°. The normalized transition time constants (Figure 3b) show a strong U-shaped trend in all but subject C. In addition, we found that the bulk of the performance increase took place with a FOV as small as 40°.

The normalized RMS values in Figure 3c show a reduction in average Stage-1 values with increasing FOV for three subjects. These data show a similar U-shaped relationship to FOV as did the T_t data. Most of the reduction in RMS error from the 10° condition takes

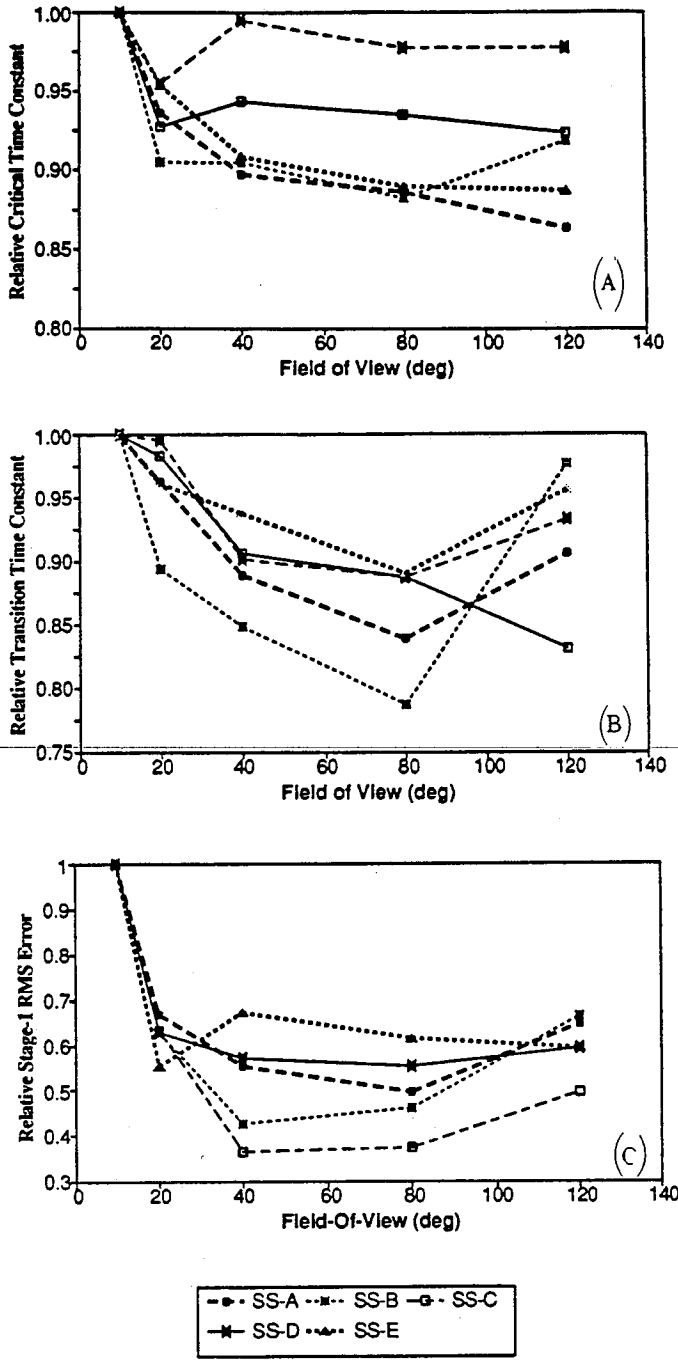

Figure 3: Normalized data vs. FOV for all subjects. (a) Critical time constant, (b) Transition time constant, (c) Stage-1 RMS

place at the 40° FOV, with the minimum RMS values between 40° to 80° FOV. Note that for subjects C and D, who showed no significant change in T_c with wider FOVs, did show significant changes in Stage-1 RMS error with widening FOV.

Discussion and Conclusion

Our data show that a small FOV of 10° or 20° does not yield as good an overall performance as can be found at 40° and beyond. The 40° FOV may encompass enough of the periphery such that image velocity can be utilized more effectively by the operator. In addition, the large changes in performance measures from 10° to 40° as compared with 40° to 120° suggest that cooperative and consistent information in both peripheral and central FOV can exert beneficial

influences for the use of visual velocity information such that moderately sized FOV can produce significant performance enhancements.

Stage-1 RMS and T_t showed an unexpected increase at 120° FOV without a commensurate increase in "effective" time delay. Our subjects' comments on comfort and ease of control more closely matched the RMS and T_t data rather than the T_c data. They reported that the task was easiest to control at 80° FOV, and noted with some amazement that the 120° FOV did not further reduce task difficulty. Thus, while subjects may be pushed by the CT paradigm to achieve a value of T_c that changes very little from 40° to 120°, the subjective reports hint that workload changes with different FOV conditions. Since a quantitative paradigm to measure workload was not included in this study, further exploration of this issue must be addressed by future experiments wherein workload is measured quantitatively.

Perhaps a factor in the increased task difficulty experienced by our subjects in the 120° FOV condition is the vection reported by our subjects in this case. Subjects reported intermittent and unpredictable episodes of vection during the conduct of these experiments, but only at the 120° FOV condition. They reported that the vection was most likely to occur at the lower λ values when the roll velocity was relatively slow, and the amplitude was low. The fact that vection reports were primarily limited to the 120° FOV condition may be due to the demanding tracking task performed by our subjects. Dichgans and Brandt [2] found that consistent vection was experienced with FOV of 60° or greater. Therefore we would have expected vection at 80° as well as 120°. However, our subjects' focus on the central field task may have suppressed vection sensations until a wider FOV produced a signal that was too strong to be suppressed by the concentration on the central task. We speculate that this intermittent vection might have disrupted the subject's concentration, thereby making the task more difficult to control. For example, the conflict between visual motion and vestibular no-motion information could lead to disorientation of the subject for brief periods, enough to distract him from the tracking task. If this were the case, then the rise in RMS error we found at 120° would be an experiment specific degradation due to the absence of true motion of the subject. One would not expect to find this behavior under conditions where veridical vestibular motion was present, but it might appear in other wide FOV no motion conditions such as fixed-based flight simulators.

Acknowledgements

The experiments were performed at: Man–Vehicle Laboratory, Department of Aeronautics and Astronautics, Massachusetts Institute of Technology, Cambridge. The authors thank Alan Natapoff for his help with the statistics and the design of the balanced trial presentations; Nick Lambropoulos for his help in analyzing some of the data; our subjects for giving so generously of their time; Larry Young and Greg Zacharias for their comments during the experiments. This work was supported by USAF contract #F33615-83-0603-0020.

References

[1] G. Andersen and M. Braunstein, Induced self-motion in central vision. J. Exp. Psychol.: Human Percpt. Perf., 11, 122-132, 1985.

[2] J. Dichgans and T. Brandt, Visual-vestibular interaction: Effects on self-motion perception and postural control. In: *Handbook of Sensory Physiology. Vol. III. Perception.* R. Held, H. Liebowitz and H. Teuber (eds.), Springer-Verlag, Berlin, 1978.

[3] R. Held, Two modes of processing spatially distributed visual stimulation. In: *The Neurosciences, Second Study Program..* F.O. Schmidt (ed.), Rockefeller University Press, New York, 1970.

[4] R. Hosman and J. van der Vaart, Effects of vestibular and visual motion perception on task performance. Acta Psychologica, 48, 271-287, 1981.

[5] E. Howlett, *Wide Angle Photography Method and System*, U.S. Patent #4,406,532, September 27, 1983.

[6] I. Howard, *Human Visual Orientation.* John Wiley and Sons, Toronto, 1982.

[7] H. Jex, J. McDonnell and A. Phatak, A Critical Tracking Task for Man-Machine Research Related to the Operator's Effective Time Delay. Part I: Theory and Experiments with a First-Order Divergent Control Element, NASA CR-616 (NTIS # N66-39893), 1966.

[8] A. Junker and D. Price, Comparison between peripheral display and motion information on human tracking about the roll axis. Proceedings AIAA Visual and Motion Simulation Conf, pp 26-28, April 1976.

[9] W. Levison and A. Junker, A model for the pilot's use of motion cues in roll axis tracking tasks. AMRL-TR-77-40 (NTIS # ADA-043-690), April 1977.

[10] T. Sheridan, W. Ferrell, *Man-Machine Systems*, MIT Press, 1974.

[11] S. Siegel, *Nonparametric Statistics for the Behavioral Sciences.* McGraw-Hill, New York, 1956.

[12] R. Shirley and L. Young, Motion cues in man-vehicle control, IEEE Trans. Man-Machine Systems, MMS-9, 121-128, 1968.

[13] W. Waespe and V. Henn, Neuronal activity in the vestibular nuclei of the alert monkey during vestibular and optokinetic stimulation. Exp. Brain Res. 27, 523-538, 1977.